Thermal Waves, Criticality, and Self-Organization in Excitable Media

P. Jung*

Department of Physics and Center for Complex Systems Research, University of Illinois at Urbana-Champaign, Urbana, Illinois 61801

(Received 7 June 1996)

Thermal waves are noise-sustained excitation patterns in excitable media coupled to a thermal environment. The coherence and spatiotemporal organization of thermal waves is quantitatively analyzed by utilizing the novel method of coherent space-time clusters. As our main result we find for strongly correlated thermal fluctuations a power-law scaling of the cluster-size distribution with a universal exponent—the fingerprint of self-organized criticality. [S0031-9007(97)02454-X]

PACS numbers: 64.60.Lx, 03.40.Kf, 05.40.+j, 47.54.+r

Pattern formation in excitable media is an important paradigm with many applications in biology and medicine such as contraction waves on the cardiac muscle, slime mold aggregation patterns, and cortical depression waves to name only a few (for an overview, see [1]). While most theoretical and experimental work is focused on the propagation of spiral waves, the role of thermal fluctuations for pattern selection and propagation has been studied only recently [2] by using a stochastic cellular model. A number of interesting phenomena such as thermal nucleation of patterns and noise controlled large-scale patterns have been found in those previous studies.

In the first part of this Letter, we report on thermal patterns, i.e., patterns which exist only in the presence of fluctuations. The common feature of patterns in fluctuating media is the stochasticity of their shapes. In the second part, we introduce a method, which enables us to *quantitatively describe* patterns with stochastic features in terms of their statistical properties. In the third part, we apply this method to thermal waves, revealing interesting properties such as criticality and in the *adiabatic limit* self-organized criticality [3].

The model.—The model, which we adopt in this Letter, consists of a square array of excitable threshold elements with lattice constant a. Each element e_{ij} can assume three states: the quiescent state, the excited state, and a following refractory state. The state of each element e_{ij} is controlled by an input $x_{ij}(t)$. If the input $x_{ij}(t)$ is below a threshold b, the element is quiescent. If $x_{ij}(t)$ is crossing threshold from below, the element switches into the excited state, i.e., it fires. The inputs $x_{ij}(t)$ are coupled to a homogeneous thermal environment, i.e., its time dependence is described by the Langevin equation

$$\dot{x}_{ij} = -\gamma x_{ij} + \sqrt{\gamma\sigma^2}\xi_{ij}(t) + \sum_n f_{ij}(t)\delta(t - t_n), \quad (1)$$

with $\langle x_{ij}^2\rangle = \sigma^2$ and zero-mean, uncorrelated noise in space and time $\langle \xi_{ij}(t)\xi_{kl}(t')\rangle = 2\delta_{(ij),(kl)}\delta(t - t')$. The excitable elements communicate via pulse coupling. When an element e_{kl} fires, it emits a spike which is received by an element e_{ij} with an intensity depending on the distance $r_{(ij),(kl)}$ between e_{kl} and e_{ij}. The spikes, sent out by firing elements e_{kl} at time $t_{n-1} = (n - 1)\Delta t$ (Δt is the smallest time scale in our model), are received by the elements e_{ij} at time t_n, yielding the additional input pulse in Eq. (1) with the weight $f_{ij}(t)$ given by

$$f_{ij}(t) = k \sum_{kl(t-\Delta t)} \exp\left(-\lambda \frac{r_{(ij),(kl)}^2}{a^2}\right). \quad (2)$$

This additional input is time dependent via the time-dependent selection of firing elements e_{kl}, indicated in Eq. (2) by the time dependence of the summation index. The parameter λ describes the inverse range of the interaction and the parameter K the coupling strength. The medium is updated synchronously in time steps of the smallest time scale Δt, being the time interval of firing. All other time scales are measured in units of Δt. The proper normalization of this model is given by $\sigma^2 \to \sigma^2/b^2, \gamma \to \gamma\Delta t, K \to K/b$ [2]. The time step as well as the threshold is therefore normalized to unity. The dissipation constant γ defines the typical time scale of the temporal evolution of a single element. For large dissipation ($\gamma > 1$), the element forgets its prehistory within one time step of temporal evolution, while for small dissipation $\gamma \ll 1$, the system—as a whole—can build up a long memory. Throughout this Letter we have used an inverse interaction range of $\lambda = 0.1$, and a refractory period of $4\Delta t$.

Subthreshold and superthreshold patterns.—It has been demonstrated [2] that this model shows for large coupling K (in the absence of noise) the typical excitation patterns of excitable media, i.e., rotating spiral waves or target waves, usually described in terms of reaction diffusion equations with two species [1]. In the presence of noise, the typical excitation patterns can still be observed, but they exhibit rough wave fronts and—depending on the noise level—more serious imperfections such as break up of wave fronts and collisions with noise-nucleated waves. The overall picture in the large coupling regime is the coexistence of multiple finite-sized cells with coherent patterns.

For weak coupling K, however, the discrete nature of the model becomes important and different phenomena

can be observed. This is the regime we are mostly concerned with in this Letter. To maintain a firing pattern, the coupling K has to exceed a critical value K_0 which is estimated for small λ and negligible curvature effects as follows: An infinite front of firing elements reduces the firing threshold of an element next to the front by an amount of S_0 which is the sum of the contributions from all firing elements along the front. The element, however, is precharged by the sum of the contributions S_{pre} of firing elements of the front at earlier times (and larger spatial distances). At the critical coupling, the sum of the precharge S_{pre} and S_0 of an element right before the front is unity (the normalized threshold), i.e.,

$$K_0(\gamma) \approx \sqrt{\frac{\lambda}{\pi}} \times \frac{1}{\exp(-\lambda) + \exp(\gamma)\sum_{n=2}^{\infty}\exp(-\lambda n^2 - n\gamma)}. \quad (3)$$

For $K < K_0$, all excitation patterns are transient to die out. In the presence of fluctuations, however, locally coherent structures with finite lifetimes emerge after a transient time. A sequence of snapshots is shown in Fig. 1 for $\gamma = 0.05$ and $K = 0.07 < K_0 \approx 0.09$. In Fig. 1(b), one can observe the spontaneous formation of a curved wave front which resembles the core of a spiral wave. In the subsequent snapshots, one can observe the propagation of the front and its eventual disappearance [Fig. 1(d)].

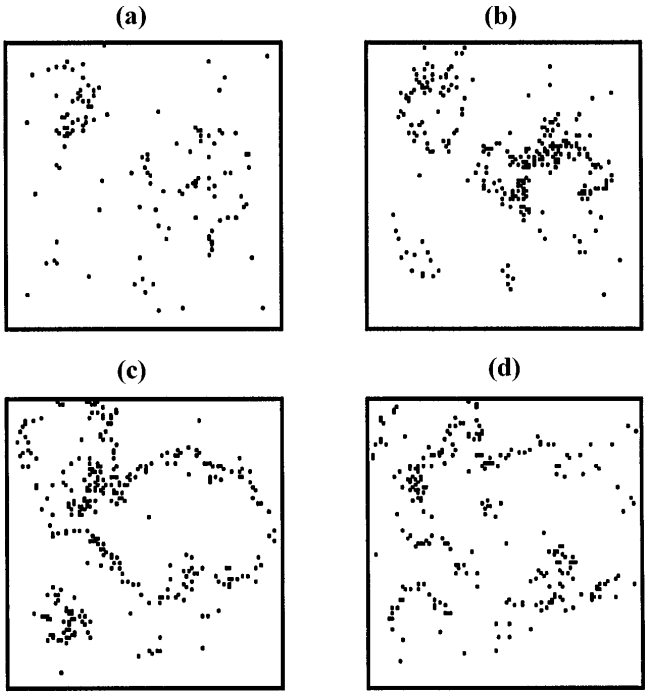

FIG. 1. Snapshots of evolving patterns are shown for $K = 0.07$, $\sigma^2 = 0.15$, $\gamma = 0.05$. The snapshots have been taken equidistantly after a transient time of about 1000 time steps with eight time steps between two consecutive snapshots. The time is progressing from (a) to (d). The array consists of 100×100 elements.

Space-time cluster analysis.—To quantitatively analyze the spatiotemporal properties of thermal waves, we introduce here a novel method based on the analysis of coherent space-time clusters. In a first step, we stack the temporal sequence of N_t snapshots of the medium taken at times $t_n = n\Delta t$ to obtain a large space-time cube which carries all the spatiotemporal information within the time interval $N_t\Delta t$. In the second step, we draw a small cube around each firing element with a spatial side length d_s and a temporal side length d_t. Overlapping small cubes in a *time-forward direction* forms objects which we have termed *coherent space-time clusters*. If two thermal waves are colliding to form one new wave after the collision, the coherent cluster corresponding to one of the incoming waves is terminated at the collision. The size s of the coherent clusters, i.e., the number of firing elements whose small cubes build the cluster, is statistical and characterized by the cluster-size distribution function $p(s, t)$. The time dependence indicates that the distribution can change with time before a steady-state distribution is approached. The particular choice of the spatial and temporal side length d_s and d_t, respectively, allows one to analyze the patterns on adjustable scales. In this Letter, we have chosen the spatial side length d_s such that the cubes of neighboring firing elements in space are overlapping, e.g., $d_s = 1.3a$ where a is the lattice constant. The temporal side length is chosen such that only the cubes of those firing elements overlap whose firing *is likely* to be causally related, e.g., $d_t = 1$ (the normalized time step).

Numerical results.—In Fig. 2, the cluster-size distributions are shown for $K = 0.07$, $\gamma = 0.05$, and $\sigma^2 = 0.15$. For small times, $t = 10, \ldots, 60$ ($N_t = 50$) (filled squares), the cluster-size distribution decays exponentially with increasing cluster sizes, indicating statistical independence of firing events. At later times (empty squares), regardless of the initial conditions, a remarkable reorganization takes place, which manifests itself by the formation of large clusters and a cluster-size distribution which scales like a power law, i.e., $p(s) \propto s^{-\alpha}$. The exponent α of the cluster-size distribution is almost independent on the variance of the noise within a wide range. The observed variations are within the accuracy of the simulations. At a *finite* value of the dissipation rate γ, there is a critical noise strength $\sigma_c^2(\gamma)$, below which neither thermal patterns nor power-law scaling of the cluster sizes can be observed. Furthermore, the power-law scaling of the cluster-size distribution is corrupted at large noise by an exponential cutoff, where the cutoff size is smaller than the system size. Decreasing the dissipation rate, i.e., $\gamma \to 0$, however, the critical noise strength $\sigma_c^2(\gamma)$ approaches zero and the power law is limited only by the finite system size (see Fig. 3)—being the linear extension

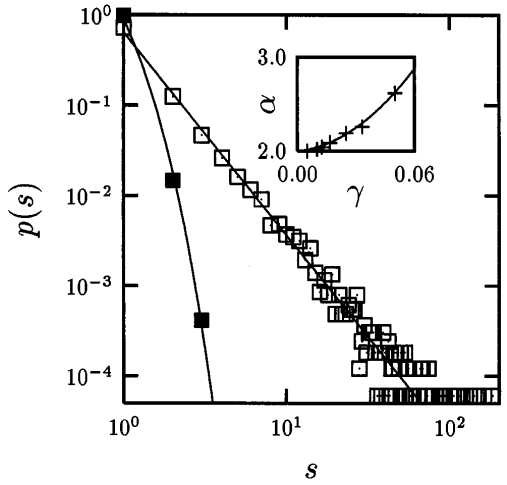

FIG. 2. The cluster-size distributions are shown for $K = 0.07$, $\sigma^2 = 0.15$, and $\gamma = 0.05$ during the initial interval of the first 50 time steps (filled squares) and a later time interval (between 800 and 850 time steps), where the system has reached its steady state (empty squares). The lines through the symbols (actual simulation results) represent an exponential fit $p(s) \propto \exp(-s/s_0)$ for the initial time interval and a power-law fit $p(s) \propto s^{-\alpha}$ for the steady-state interval. The inset shows the exponent α as a function of the dissipation rate γ at constant variance of the noise $\sigma^2 = 0.15$. The solid curve is fitted through the numerical data points (crosses) to guide the eye. The array used for the calculations consists of 200×200 elements.

of the array due to the slimness of the clusters. In the inset of Fig. 2, the exponent α is shown as a function of the dissipation rate γ at constant variance of the noise $\sigma^2 = 0.2$. For decreasing γ, the exponent α approaches $\alpha_0 = 2$ from above.

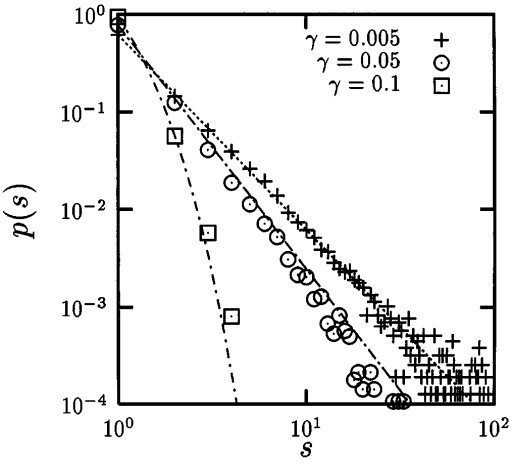

FIG. 3. The normalized cluster-size distribution is shown for several dissipation rates γ at constant variance of the noise $\sigma^2 = 0.2$. For $\gamma = 0.005$ and 0.05, we have fitted a power law through the points at small cluster sizes. The deviations from this line at large cluster sizes (cutoff) is visible at $\gamma = 0.05$. The line through the points for $\gamma = 0.1$ represents an exponential fit. The array used for the calculations consists of 200×200 elements.

Self-organized criticality—The power-law scaling of the cluster-size distribution suggests the picture of an avalanche process rather than the propagation of a nonlinear wave. Avalanche processes where the size of the avalanches scales with a power law have been reported in quite a variety of systems such as in earthquake observations and models [4], flux creep in type II superconductors [5], domain-wall motion in ferromagnets [6], and ricepiles [7]. Many of these experimental results are being discussed in terms of the concept of self-organized criticality, put forward by Bak and collaborators [3]. The characteristic features of self-organized criticality are (a) power-law distributed size of fluctuations and (b) self-tuning into criticality. An essential feature of the sandpile automata [3] and also later models (such as the Bak-Sneppen model for biological evolution) is that the avalanches happen instantaneously on the time scale of the perturbation, externally imposed on the system (e.g., a grain of sand thrown on the sandpile). This separation of time scales is not a general feature of our model. The system evolves and all sites are affected by local fluctuations during an avalanche. As observed from the numerical simulations, criteria (a) and (b) for self-organized criticality are not fulfilled for finite values of the dissipation rate γ since tuning of the noise to σ_c^2 is necessary to obtain power-law distributed cluster sizes. This noise tuning, however, appears not necessary in the limit of vanishing dissipation $\gamma \to 0$ where the cutoff size strongly increases and the critical noise strength σ_0^2 approaches 0. Here criteria (a) and (b) for self-organized criticality are fulfilled. The significance of the limit $\gamma \to 0$ is that time-scale separation of local dynamics and avalanche dynamics is reinstalled. Local dynamics consists of dissipation with rate γ and thermal activation to the excited state with a mean activation time $T_{ac} \propto \exp(1/2\sigma^2)$. The conditions for time-scale separation are that the activation time T_{ac} and the relaxation time γ^{-1} have to be larger than the longest possible duration of an avalanche being roughly estimated in dimensionless units by the linear extension L of the array (a wave front moves one lattice constant per time interval and shows no significant rotation). For the parameters used in Fig. 3, i.e., $\sigma^2 = 0.2$ and $L = 200$, the relevant condition for time-scale separation $\gamma < 1/L = 0.005$ is compatible with the observation that the cutoff of the power-law distribution has disappeared at $\gamma = 0.005$. Furthermore, the exponent of the power-law distributed cluster sizes is close to $\alpha_0 = 2$ within the regime of time-scale separation. This means that the system is—as it should be for a system in a critical state—long-range correlated. The *super universal* exponent $\alpha_0 = 2$ has been reported on [8] for the scaling of the size distribution of time-forward avalanches in models for invasion percolation [9] and biological evolution [10].

Coherent cluster method vs avalanche statistics.—The above discussed connection of our model and self-organized criticality raises the question in how far

avalanche statistics, mostly used in the context of self-organized criticality, is related to the method of coherent clusters introduced in this Letter. In the following, we list a number of differences in the procedure and scope.

(1) The method of coherent clusters is not particularly tailored to explore critical properties of a spatially extended systems. *Any* spatiotemporal pattern (after a suitable binary reduction) can be analyzed and characterized with this method.

(2) The possibility of varying the spatial and temporal side length of the small "space-time cubes" around each active element allows us to scan the structure of the coherent clusters on *different space and time scales,* to, e.g., measure their fractal properties.

(3) Coherent cluster analysis allows multiple clusters at the same time. This is particularly important for analyzing experimental spatiotemporal patterns [11].

In conclusion, patterns in excitable media coupled to a thermal environment have been analyzed by using a novel technique—the method of coherent space-time clusters. Our focus was on noise-sustained thermal patterns which do exist only in the presence of fluctuations. We have found that for *slow* local dynamics, the medium emerges into a critical state where thermal waves represent power-law distributed fluctuations. The exponent of the power law is found to be $\alpha_0 = 2$ in agreement with those of time-forward avalanches of other self-organizing systems such as invasion percolation or the Bak-Sneppen model for biological evolution. We believe that the link between the dynamics of excitable media and self-organized criticality, presented in this Letter, could have quite interesting consequences for a number of biological systems with excitable dynamics such as neuronal assemblies and cortical tissue. In a very recent experiment [11], the method of coherent space-time clusters, presented here for the first time, has been applied to analyze the spatiotemporal properties of chemical waves on clusters of hippocampal astrocytes. As in the model discussed here, power-law distributed clusters have been found with the universal exponent around $\alpha = 2$ (variations due to experimental inaccuracies)—a strong hint that self-organized criticality in excitable media plays a relevant role for brain functions.

I want to express my gratitude to Kurt Wiesenfeld for drawing my attention to recent papers on punctuated equilibrium. Valuable discussions with Maya Paczuski and Stefan Boettcher on some issues on self-organized criticality are highly appreciated. This work has been supported by the Deutsche Forschungsgemeinschaft within the Heisenberg program.

*Present address: School of Physics, Georgia Institute of Technology, Atlanta, GA 30332.

[1] J. D. Murray, *Mathematical Biology* (Springer-Verlag, Berlin, 1989).
[2] P. Jung and G. Mayer-Kress, Chaos **5**, 458 (1995); P. Jung and G. Mayer-Kress, Phys. Rev. Lett. **74**, 2130 (1995).
[3] P. Bak, C. Tang, and K. Wiesenfeld, Phys. Rev. Lett. **59**, 381 (1987).
[4] B. Gutenberg and C. F. Richter, Ann. Geofis. **9**, 1 (1956); P. Bak and C. Tang, J. Geophys. Res. B **94**, 15 635 (1989); J. Carlson and J. Langer, Phys. Rev. Lett. **62**, 2632 (1989).
[5] S. Field, J. Witt, F. Nori, and Xingshen Ling, Phys. Rev. Lett. **74**, 1206 (1995).
[6] X. Che and H. Suhl, Phys. Rev. Lett. **64**, 1670–1673 (1990); H. Suhl, J. Applied Phys. **69**, 5447 (1991).
[7] V. Frette, K. Christensen, A. Malthe-Sorenssen, J. Feder, T. Jossang, and P. Meakin, Nature (London) **379**, 44 (1996).
[8] S. Maslov, Phys. Rev. Lett. **74**, 562 (1995).
[9] D. Wilkinson and J. F. Wilemsen, J. Phys. A **16**, 3365 (1983).
[10] P. Bak and K. Sneppen, Phys. Rev. Lett. **71**, 4083 (1993); M. Paczuski, S. Maslov, and P. Bak, Phys. Rev. E **53**, 414 (1996); S. Boettcher and M. Paczuski, Phys. Rev. E **54**, 1082 (1996).
[11] P. Jung, A. Cornell-Bell, K. Madden, and F. Moss (unpublished).